Article

Intramolecular Photoinduced Charge Transfer in Rotaxanes

Phoebe H. Kwan, and Timothy M. Swager

J. Am. Chem. Soc., **2005**, 127 (16), 5902-5909• DOI: 10.1021/ja042535o • Publication Date (Web): 15 March 2005

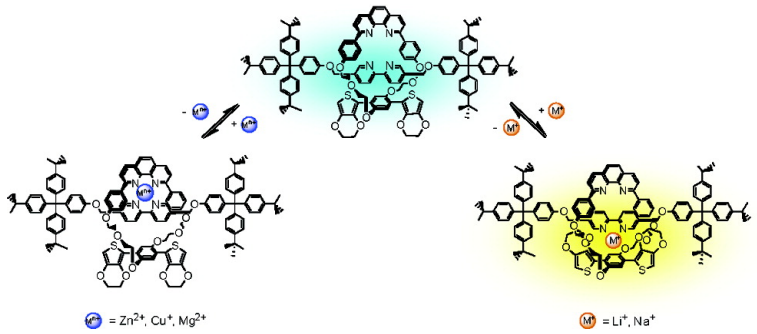

More About This Article

Additional resources and features associated with this article are available within the HTML version:

- Supporting Information
- Links to the 9 articles that cite this article, as of the time of this article download
- Access to high resolution figures
- Links to articles and content related to this article
- Copyright permission to reproduce figures and/or text from this article

View the Full Text HTML

J|A|C|S
ARTICLES
Published on Web 03/15/2005

Intramolecular Photoinduced Charge Transfer in Rotaxanes

Phoebe H. Kwan and Timothy M. Swager*

Contribution from the Department of Chemistry, Massachusetts Institute of Technology, Cambridge, Massachusetts 02139

Received December 13, 2004; E-mail: tswager@mit.edu

Abstract: We report the synthesis and photophysical investigation of a series of rotaxanes in which the physical confinement of the donor and acceptor (DA) pair leads, in some cases, to emissive exciplexes. As a comparison, we examined the photoinduced charge-transfer processes in the same DA mixtures under intermolecular conditions. The interlocked configuration of the rotaxane facilitates π orbital overlap of the excited state DA pair by keeping their center-to-center distance extremely small. This increased interaction between the DA pair significantly lowers the activation energy for exciplex formation (E_a) and helps stabilize the highly polar charge-transfer complex. We find that the stabilizing effect of the rotaxane architecture compensates for the modest thermodynamic driving force for some charge-transfer interactions. In addition, we examined the temperature dependence on the rotaxanes' optical properties. Metal coordination to the tetrahedral cavity disrupts the cofacial conformation of the DA pair and quenches the fluorescence. Binding of alkali metal ions to the 3,4-ethylenedioxythiophene (EDOT)-based rotaxane, however, gives rise to the emergence of a new weak emission band at even lower energies, indicative of a new emissive exciplex.

Introduction

Interactions between an electron donor and an acceptor sometimes lead to complex photophysical and/or photochemical phenomena. A donor−acceptor (DA) interaction in the ground state gives rise to a charge-transfer (CT) complex, characterized by the emergence of a new absorption band at lower energies. An exciplex results from a bimolecular interaction of an excited donor with a ground-state acceptor, and vice versa. While both interactions quench the fluorescence of the parent molecules and occasionally give rise to new emissive species, the ground-state counterpart of an exciplex is thermodynamically unstable. This report will focus on excited-state charge-transfer complexes in rotaxanes.

Figure 1 depicts the reaction coordinate energy diagram of exciplex emission.[1] ΔE_{00} refers to the 0,0 singlet transition of the emissive molecule of interest. When a polarizable excited-state molecule encounters a polarizable ground-state molecule of a different species, they can interact and form an exciplex. This metastable complex draws most of its stabilization energy (ΔH_{ex}) from charge-transfer interactions between the two molecules; thus, we will resort to using the terms donor (D) and acceptor (A). In general, the electronic state of the exciplex, $(A^{\delta-}D^{\delta+})^*$, is a combination between the charge-transfer state, various excitation resonance, and locally excited states (LES) (sometimes including the ground state) between its constituents. Its wave function can be described as

$$\psi = c_1\psi(A^-D^+) + c_2\psi(AD)^*$$

Many exciplexes decay via nonradiative pathways. Some systems, however, exhibit emissive exciplexes. As the exciplex relaxes to the neutral ground state donor/acceptor pair, the

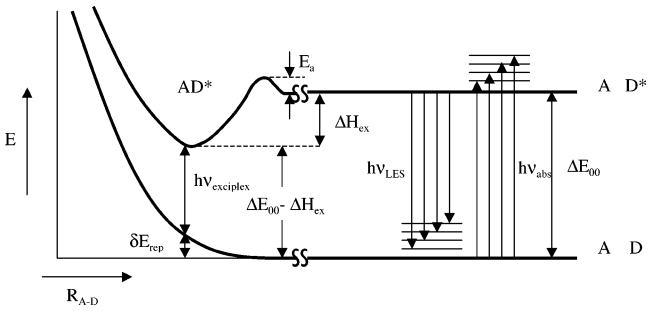

Figure 1. Surface-energy diagram for exciplex emission.

stabilization energy from charge-transfer interactions causes a red-shifted emission compared to the LES fluorescence, as well as a longer excited-state lifetime. In addition, the exciplex emission is further red-shifted by the repulsive forces, δE_{rep} of its ground-state counterpart. Since exciplex formation requires direct orbital overlap between the donor and the acceptor, it has been suggested that the optimal distance of the DA pair is between 3 and 7 Å.[2] As a result, the photophysics of an exciplex is highly sensitive to diffusion and the relative conformation of the DA pair. Diffusion-limited exciplex formation in general exhibits bimolecular reaction kinetics.[3] Furthermore, an exciplex exhibits solvatochromic fluorescence due to its highly polar nature. In systems where the LES and the $(A^{\delta-}D^{\delta+})^*$ state are close in energy, the charge-transfer step becomes reversible. In

(1) (a) Turro, N. In *Modern Molecular Photochemistry*; University Science Books: Sausalito, 1991; p 139. (b) Förster, T. *Angew. Chem., Int. Ed. Engl.* **1969**, *8*, 333.

(2) (a) Bixon, M.; Jortner, J. *J. Phys. Chem.* **1993**, *97*, 13061−13066. (b) Scully, A. D.; Takeda, T.; Okamoto, M.; Hirayama, S. *Chem. Phys. Lett.* **1994**, *228*, 32−40. (c) Kroon, J.; Verhoeven, J. W.; Paddon-Row, M. N.; Oliver, A. M. *Angew. Chem.* **1991**, *30*, 1358−1361. (d) Inai, Y.; Sisido, M.; Imanishi, Y. *J. Phys. Chem.* **1990**, *94*, 6237−6243.

10.1021/ja042535o CCC: $30.25

this case, one can vary the solvent polarity or temperature to observe dual fluorescence.[4]

Fluorescence quenching via electron transfer was originally proposed in the 1930s.[5] In the 1960s, Leonhardt and Weller reported fluorescence quenching of perylene by electron-donating (or electron-accepting) molecules.[6] In addition, they observed a new emission at longer wavelengths in nonpolar solvents. Since then, intermolecular exciplexes have been extensively studied. Examples of DA pairs include naphthalene/9,10-dicyanoanthracene,[7] naphthalenes/conjugated dienes,[8] and dimethoxybenzene/chlorobenzenes.[9] Because the excited donor must encounter and interact with a ground-state acceptor (or vice versa) within its excited-state lifetime, intermolecular exciplexes are observed only at relative high DA concentrations.

In intramolecular exciplexes, the covalent connectivity between the donor and acceptor greatly increases the effective concentration of the DA pair, and the charge-transfer step becomes unimolecular.[3] The nature of the covalent linker ranges from flexible alkyl chains[10] to rigid bridged hydrocarbons[11] to semirigid and/or helical biological moieties such as peptides and DNA.[12] By varying the length and rigidity of the linker, one could control the distance and orientation between the donor and acceptor and hence alter the exciplex's optical properties.[13]

Previously, our group reported a unique class of emissive exciplexes by confining a phenylene−ethynylene-based donor and a bipyridine diester acceptor in a rotaxane scaffold.[14] The single-crystal X-ray structure confirmed the sandwich orientation of the donor and acceptor with a cofacial distance of 3.50 Å, both attributes in favor of exciplex conformation. Furthermore, metal binding quenches the fluorescence (both exciplex and LES emission) by disrupting the sandwich conformation of the DA pair. In a subsequent report, we demonstrated that substituting the ester linkage with a methylene-ether group in the acceptor compromised its electron affinity, such that the rotaxanes showed macrocycle LES emission that can be quenched by interactions with proton donors.[15] Similar to intermolecular exciplexes, the donor and acceptor in a rotaxane retain most of their rotation and translational freedom without being covalently connected. Analogous to typical intramolecular exciplexes, the mechanical restriction of the donor and acceptor to within contact distance effectively eliminates diffusion as a limiting factor. Because of their interlocked nature, these systems lend themselves to photophysical kinetics and properties that resemble both intramolecular and intermolecular exciplexes. In this report, we examine the consequences of the mechanical confinement of the DA pair in a rotaxane to better establish the structure−property relations of the rotaxane exciplexes.

Experimental Section

Materials. $Pd(PPh_3)_4$ and *trans*-$PdCl_2(PPh_3)_2$ were obtained from Strem. *N*-methylpyrollidone (NMP), *p*-methoxyethynylbenzene, and CuI were obtained from Aldrich and used without further purification. Diisopropylamine and toluene were obtained from Aldrich and were purified by distillation from sodium prior to use. The synthesis of 2-(tributylstannyl)-3,4-ethylenedioxythiophene,[16] 5-(tributylstannyl)-2,2′-bithiophene,[17] and compounds **1**−**4**, **8**−**11**[15,18] have been described elsewhere. The threading unit **12** was isolated as a byproduct from the synthesis of rotaxane **3**.

Equipment. All reactions and manipulations were carried out under an atmosphere of inert argon or nitrogen using Schlenk techniques or in an inert-atmosphere glovebox (Innovative Technologies) unless otherwise noted. Solution 500 MHz ^{1}H NMR spectra and 125.8 MHz ^{13}C NMR spectra were recorded on a Varian Unity 500 spectrometer and were referenced to $CDCl_3$ (δ = 7.27 ppm and δ = 77.23 ppm, respectively) unless otherwise noted. UV−vis spectra were obtained in various solvents from a Cary 50 UV−visible spectrophotometer using a 1-cm quartz cuvette. Mass spectra were obtained on a Bruker Daltonics APEXII3 Tesla FT-ICR mass spectrometer using electrospray ionization. Fluorescence studies were conducted with a SPEC Fluorolog-2 fluorimeter (model FL112, 450 W xenon lamp). All emission and excitation spectra were corrected for the detector response and the lamp output. Quantum yields were referenced to quinine sulfate in 1 N sulfuric acid (Φ_F = 0.55).[19] Polymer thin films on cover glass slides (18 mm × 18 mm) were spin cast on a EC101DT Photoresist Spinner (Headway Research, Inc.) using a spin rate of 3000 rpm from chloroform solutions.

Excited-State Lifetime Experiments. The time of fluorescence decay for highly emissive compounds (QY > 0.1) was determined by a phase-modulation method[20] using frequencies from 10 to 200 MHz and using Ludox−water solutions (scattering sample, τ = 0 ns, right-angle geometry) as a standard. The experimental errors were typically 4−8% in phase angle and 1−3% in modulation. For weakly emissive species (QY < 0.1), we used a subpicosecond laser system to measure the lifetimes. The subpicosecond laser system consists of a Coherent/BMI Oomet-400S two-stage optical parametric amplifier (OPA). The OPA generates laser pulses at a repetition rate of 1 kHz and offers wavelength tenability from 475 to 710 nm with pulse energies greater than 20 μJ. The OPA is pumped by a Coherent/BMI Alpha-1000 chirped-pulse regenerative amplifier, which, in turn, is pumped by a 10-W, 1-kHz Nd:YLF laser and seeded by a Coherent Mira femtosecond Ti:sapphire oscillator. The oscillator is pumped by a 5-W cw Coherent Verdi solid-state, frequency doubled Nd:YVO_4 laser. Pulses from the regenerative amplifier can be characterized in real time by a Positive Light single-shot autocorrelator, and they were measured to be 100 fs

(3) (a) Gould, I.; Ege, D.; Moser, J. E.; Farid, S. *J. Am. Chem. Soc.* **1990**, *112*, 4290−301. (b) Cosa, G.; Chesta, C. *J. Phys. Chem. A* **1997**, *101*, 4922−4928.
(4) (a) Bangal, P. R.; Chakravorti, S. *J. Photochem. Photobiol., A*; *Chem.* **1998**, *116*, 47−56. (b) Ghoneim, N. *Spectrochim. Acta, Part A* **2001**, *57*, 483−489.
(5) (a) Bauer, E. *Z. Physik. Chem., Abt. B* **1932**, *16*, 465. (b) Weiss, J.; Fischgold, H. *Z. Physik. Chem., Abt. B* **1936**, *32*, 135.
(6) (a) Leonhardt, H.; Weller, A. *Z. Physik. Chem. Neue. Folge*. **1961**, *29*, 277−280. (b) Leonhardt, H.; Weller, A. Ber. *Bunsen-Ges. Phys. Chem.* **1963**, *67*, 791−795.
(7) (a) Kizu, N.; Itoh, M. *J. Phy. Chem.* **1992**, *96*, 5796−5800. (b) Kuz'min, M. G.; Sadoviskii, N. A.; Soboleva, I. V. *Chem. Phys. Lett.* **1980**, *71*, 232−237.
(8) Labianca, D. A.; Taylor, G. N.; Hammond, G. S. *J. Am. Chem. Soc.* **1972**, *94*, 3679−3683.
(9) Carroll, F.; McCall, M. T.; Hammond, G. S. *J. Am. Chem. Soc.* **1973**, *95*, 315−318.
(10) (a) Scherer, T.; van Stokkum, I. H.; Brouwer, A. M.; Verhoever, J. W. *J. Phys. Chem.* **1994**, *98*, 10539−10549. (b) De Schryver, F. C.; Collart, P.; Vandendriessche, J.; Goedeweeck, R.; Swinnen, A.; van der Auweraer, M. *Acc. Chem. Res.* **1987**, *20*, 159−166.
(11) Bixon, M.; Jortner, J.; Verhoeven, J. W. *J. Am. Chem. Soc.* **1994**, *116*, 7349−7355.
(12) (a) Galindo, F.; Burguete, M. I.; Luis, S. V. *Chem. Phys.* **2004**, *302*, 287−294. (b) Lewis, F. D.; Liu, J.; Weigel, W.; Rettig, W.; Kurnikov, I. V.; Beratan, D. N. *Proc. Natl. Acad. Sci. U.S.A.* **2002**, *99*, 12536-12541.
(13) For leading references, see: Vanderauwera, P.; DeSchryver, F. C.; Weller, A.; Winnik, M. A.; Zachariasse, K. A. *J. Phys. Chem.* **1984**, *88*, 2964−2970.
(14) MacLachlan, M. J.; Rose, A.; Swager, T. M. *J. Am. Chem. Soc.* **2001**, *123*, 9180−9181.
(15) Kwan, P. H.; MacLachlan, M. J.; Swager, T. M. *J. Am. Chem. Soc.* **2004**, *126*, 8638−8639.
(16) Zhu, S. S.; Swager, T. M. *J. Am. Chem. Soc.* **1997**, *10*, 5541−5545.
(17) (a) Hark, R. R.; Hauze, D. B.; Petrovslaia, O.; Joullie, M.; Jaouhari, R.; McComiskey, P. *Tetrahedron Lett.* **1994**, *35*, 7719−22. (b) Zhu, S. S.; Swager, T. M. *Adv. Mater.* **1996**, *8*, 497−500.
(18) Buey, J.; Swager, T. M. *Angew. Chem., Int. Ed.* **2000**, *39*, 608−612.
(19) Melhuish, N. Z. *J. Opt. Soc. Am.* **1964**, *54*, 183−188.
(20) (a) Hieftje, G. M.; Vogellstein, E. E. In *Modern Fluorescence Spectroscopy*; Wehry, E. L., Ed.; Plenum Press: New York, 1981. (b) Lakowicz, J. R. *Principles of Fluorescence Spectroscopy*; Plenum Press: New York, 1986.

in duration. Emission lifetimes were measured on a Hamamatsu C4334 Streak Scope streak camera, which was controlled with the high-performance digital temporal analyzer (HPDTA) software provided by Hamamatsu Photonics. This system allows for measurements of lifetimes with a resolution of ~10 ps in a time window up to 1 ms limited by the laser repetition rate. For our systems, delays (<100 ns) were generated by a Hamamatsu C1097-04 delay unit. The streak camera is capable of measuring the rise and decay of fluorescence at every wavelength in a 100-nm window simultaneously, allowing for a direct comparison of the kinetics of different spectral features. In this study, the samples were excited using the 650-nm output from the OPA, which was then frequency doubled to generate 325 nm pulses, and emission was collected with the spectral window centered at the emission maxima of the compound of interest.

Synthesis of Rotaxane 5. In a 25-mL Schlenk flask under Ar, rotaxane **1** (100 mg, 0.049 mmol), 27 mg (0.14 mmol) of CuI, 2 mL of toluene, and 1 mL of $^{i}Pr_2NH$ were combined. The solution was purged with argon for 30 min, at which time 10 mg (0.009 mmol) of $Pd(PPh_3)_4$ and 80 μL (0.62 mmol) of *p*-methoxyethynylbenzene were added. The mixture was stirred at 60 °C for 24 h and then evaporated to dryness. The contents were dissolved in 100 mL of CH_2Cl_2 and washed with 100 mL of H_2O plus ca. 65 mg of KCN. The organic layer was washed with 2 × 100 mL of H_2O and brine and then filtered. Following chromatography on SiO_2, eluting byproducts/starting material with CH_2Cl_2, the product was eluted with 1:9 ethyl acetate:CH_2Cl_2. Recrystallization by slow diffusion of MeCN layered onto a solution of the crude product in CH_2Cl_2 afforded **5** as light-yellow crystals (78 mg, 78%).

Data for 5: ^{13}C NMR (125.8 MHz, $CDCl_3$) δ = 160.25, 157.10, 156.89, 153.71, 148.91, 148.75, 146.74, 145.04, 140.56, 136.95, 133.51, 133.32, 132.37, 130.89, 129.50, 127.97, 126.10, 124.78, 121.21, 120.06, 117.68, 115.70, 115.39, 114.51, 114.13, 95.76, 70.24, 70.00, 68.09, 67.91, 63.58, 55.75, 34.69, 31.61 ppm. ^{1}H NMR (499.8 MHz, $CDCl_3$) δ = 8.34 (s, 2H), 8.02 (d, J = 9 Hz, 2H), 7.97 (d, J = 8.5 Hz, 2H), 7.84 (d, J = 9 Hz, 4H), 7.73 (d, J = 8.5 Hz, 2H), 7.529 (s, 2H), 7.50 (dd, J = 8 Hz, 2 Hz, 2H), 7.08 (d, J = 9 Hz, 4H), 6.98 (d, J = 8.5 Hz, 6H), 6.88 (d, J = 8.5 Hz, 6H), 6.85 (s, 2H), 6.59 (d, J = 10 Hz, 4H), 6.55 (d, J = 6.5 Hz, 2H), 6.52 (d, J = 9 Hz, 2H), 5.10 (s, 2H), 4.62 (q, J = 11.5, 4H), 3.97 (m, 4H), 3.93 (m, 2H), 3.82 (m, 2H), 3.70 (m, 12H), 3.47 (s, 6H), 1.08 (s, 54H) ppm. HRMS m/z = 2064.39 ([M + H]$^+$) (calcd m/z = 2064.67).

Synthesis of Rotaxane 6. In a 25-mL Schlenk flask under Ar, rotaxane **1** (0.337 g, 0.164 mmol), CuI (0.096 g, 0.504 mmol), and 2-(tributylstannyl)-3,4-ethylenedioxythiophene (0.300 g, 0.694 mmol) were combined. The mixture was dissolved in 10 mL of *N*-methylpyrollidone (NMP). The solution was purged with argon for 15 min, at which time $Pd(PPh_3)Cl_2$ (6 mg, 5 mol %) was added to the reaction mixture. The reaction was stirred at 100 °C for 18 h, and then solvent was removed in vacuo. The residue was dissolved in 100 mL of CH_2Cl_2. The organic layer was washed with 2 × 100 mL of 0.1 M KCN solution, affording a light-beige solution, followed by 100 mL of H_2O and 100 mL of KF solution and brine. The collected organic layer was dried over Na_2SO_4 and filtered. The solution was concentrated and purified using column chromatography. One drop of triethylamine was added in the solvent to prevent proton-assisted oxidation of the product. Following chromatography on SiO_2, eluting byproducts/starting material with CH_2Cl_2, the thread **13** was eluted with 5:95 ethyl acetate:CH_2Cl_2. After that, the product was eluted with 1:9 ethyl acetate:CH_2Cl_2. Recrystallization by slow diffusion of MeCN layered onto a solution of the crude product in CH_2Cl_2 afforded **6** as light-yellow crystals (0.274 g, 80% yield).

Data for 6: ^{13}C NMR (125.8 MHz, CD_2Cl_2) δ = 160.29, 156.89, 148.98, 148.77, 146.67, 145.07, 141.74, 140.45, 139.44, 136.97, 133.16, 132.95, 132.31, 130.89, 129.43, 127.96, 126.08, 124.78, 121.42, 121.07, 119.88, 115.43, 114.07, 113.31, 100.18, 70.22, 70.02, 69.61, 68.05, 67.76, 65.28, 64.61, 63.57, 34.70, 31.62 ppm. ^{1}H NMR (500.3 MHz, $CDCl_3$) δ = 8.47 (s, 2H), 8.15 (d, J = 13.5 Hz, 2H), 8.13 (d, J = 14.5 Hz, 4H), 8.06 (d, J = 13.5 Hz, 2H), 7.91 (d, J = 14.0 Hz, 2H), 7.67 (s, 4H), 7.58 (d, J = 13.5 Hz, 2H), 7.18 (d, J = 14.0 Hz, 4H), 7.03 (d, J = 14.0 Hz, 4H), 7.00 (d, J = 13.5 Hz, 2H), 6.80 (d, J = 15.0 Hz, 2H), 6.73 (d, J = 15.0 Hz, 2H), 6.21 (s, 2H), 4.77 (q, J = 19.5 Hz, 4H), 4.38−4.28 (m, 2H), 4.24−4.09 (m, 2H), 4.06−3.76 (m, 12H), 1.27 (s, 54H). HRMS m/z = 2084.39 ([M + H]$^+$) (calcd m/z = 2084.79).

Data for 12. This compound is only marginally soluble enough in $CDCl_3$ for ^{1}H NMR but too insoluble for ^{13}C NMR. ^{1}H NMR (499.8 MHz, $CDCl_3$) δ = 9.47 (d, J = 2.0 Hz, 2H), 8.70 (d, J = 8.0 Hz, 2H), 8.61 (dd, J = 8.0 Hz, 2 Hz, 2H), 7.26 (overlapped with solvent peak, theoretically 12H), 7.24 (d, J = 8.5 Hz, 4H), 7.13 (d, J = 8.5 Hz, 12H), 7.08 (d, J = 8.5 Hz, 4H), 1.30 (s, 54H) ppm.

Synthesis of Rotaxane 7. Rotaxane **7** was prepared using a procedure and purification analogous to that for **6**. Based on 100 mg (0.049 mmol) of rotaxane **1** and 151 mg (0.33 mmol) of 5-(tributylstannyl)-2,2′-bithiophene, 92 mg (89%) of rotaxane **7** was obtained as a bright-yellow solid.

Data for 7: ^{13}C NMR (125.8 MHz, CD_2Cl_2) δ = 160.29, 148.73, 148.66, 146.69, 145.08, 132.25, 130.87, 129.45, 128.41, 126.65, 126.06, 124.79, 124.70, 124.02, 123.78, 120.96, 115.55, 114.01, 70.22, 68.09, 34.69, 31.62 ppm. ^{1}H NMR (500 MHz, CD_2Cl_2) δ = 8.32 (s, 2H), 8.12 (d, J = 8.5 Hz, 2H), 8.00 (d, J = 8 Hz, 2H), 7.93 (d, J = 8.5 Hz, 4H), 7.83 (d, J = 8.5 Hz, 2H), 7.63 (s), 7.46 (d, J = 6 Hz, 2H), 7.17 (d, J = 4 Hz, 2H), 7.10 (d, J = 8.5 Hz, 12H), 7.03 (dd, J = 5 Hz, 0.5 Hz, 2H), 6.99 (d, J = 8.5 Hz, 12H), 6.96 (s, 2H), 6.91 (d, J = 8.5 Hz, 4H), 6.84 (dd, J = 5 Hz, 4 Hz, 2H), 6.79 (d, J = 4 Hz, 2H), 6.71 (d, J = 9 Hz, 4H), 6.51 (d, J = 9 Hz, 4H), 4.63 (d, J = 12 Hz, 2H), 4.53 (d, J = 12 Hz, 2H), 4.31 (m, 2H), 4.21 (m, 2H), 4.00 (m, 4H), 3.94 (m, 2H), 3.87 (m, 2H), 3.83 (m, 4H), 1.11 (s, 54H) ppm. HRMS m/z = 2132.29 ([M + H]$^+$) (calcd m/z = 2132.88).

Results and Discussion

We synthesized a series of Sauvage-type[21] rotaxanes (Chart 1) with four different donors and two acceptors (Chart 2). Macrocycles **8** and **9** contain phenylene−ethynylene-based units, while macrocycles **10** and **11** bear conjugated aryl thiophene derivatives. These four compounds made up the array of emissive donors of different electron-donating ability. The nonemissive acceptors are composed of the bipyridine diester or bipyridine diether threading units (**12** and **13**, respectively). Previously, we reported the syntheses of rotaxanes **2**, **3**, and **4** via Sonogashira−Hagihara cross coupling.[14,15] We applied the same methodology to prepare rotaxane **5**, with 4-ethynylanisole as the starting material. The reaction of diiodorotaxane **1** with the respective organostannanes via Stille cross-coupling provided the thiophene-based rotaxanes (**6** and **7**) in respectable yields (Scheme 1). In the cross-coupling reactions the role of copper iodide is 2-fold[14] as a catalyst and as a tight-binding guest (Cu^+ ion) in the cavity to avoid deactivation of the palladium catalyst. The complexes are isolated in metal-free form due to the fact that the copper ion is removed by aqueous cyanide extraction in the reaction workup.

UV−vis Absorption and Emission Studies. Table 1 lists the fluorescence properties of the rotaxanes and the macrocycle donors. The absorption spectra of all rotaxanes reflected the additive absorption profiles of their respective donors and acceptors (Figure 2). The nonexciplex rotaxanes **4**, **5**, and **7** exhibited emission essentially identical to those from their

(21) (a) Dietrich-Buchecker, C. O.; Sauvage, J. P.; Kintzinger, J. P. *Tetrahedron Lett.* **1983**, *24*, 5095. (b) Dietrich-Buchecker, C. O.; Sauvage, J. P.; Kern, J. M. *J. Am. Chem. Soc.* **1984**, *106*, 3043. (c) Jimenez-Molera, M. C.; Dietrich-Buchecker, C.; Sauvage, J. P. *Chem. Eur. J.* **2002**, *8*, 1456.

Chart 1

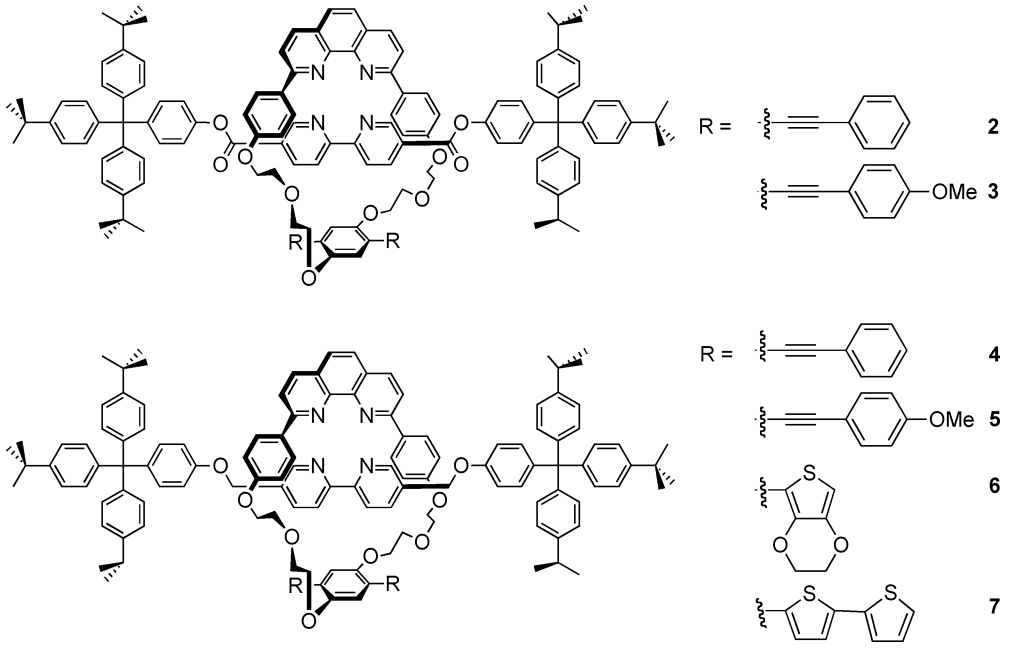

Chart 2

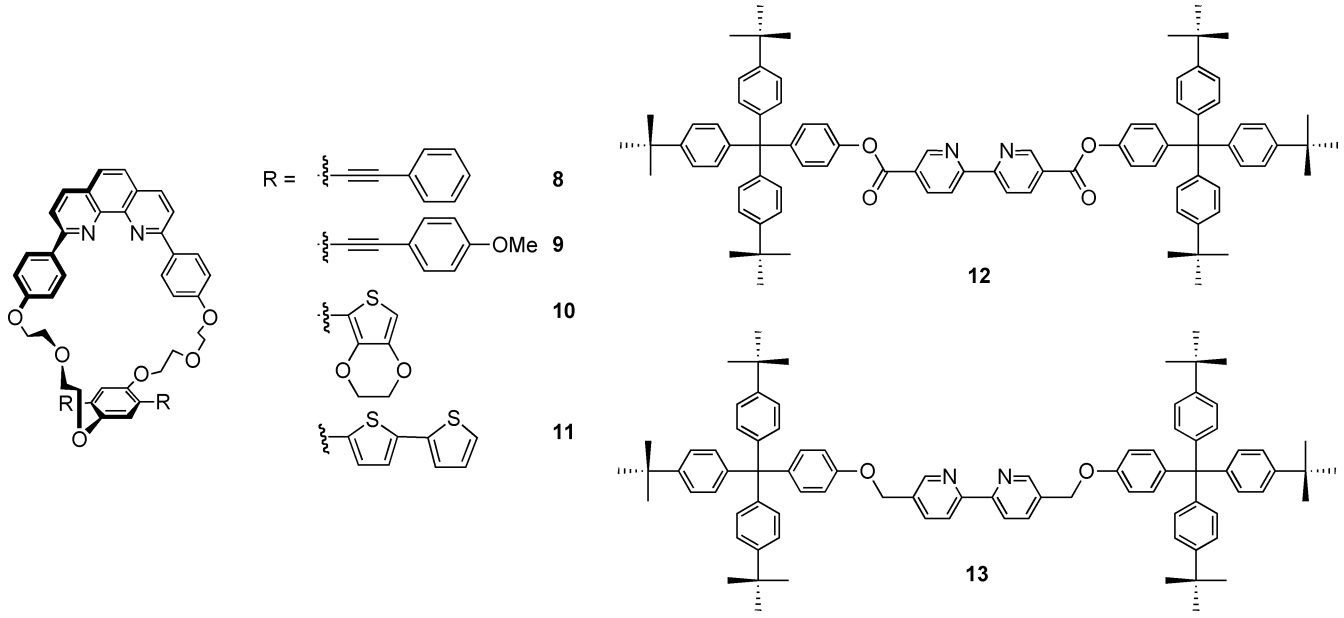

respective LES macrocyclic donors. Rotaxanes **2**, **3**, and **6**, on the other hand, revealed broad and featureless emission bands at lower energies. The exciplex emission band consists of a series of unresolved peaks separated by the average vibrational energy, $h\nu_v$ and are subjected to Gaussian broadening by the solvent reorganization energy, λ_s. In addition, the rotaxane exciplexes showed lower quantum yields and the expected longer excited-state lifetimes compared to their respective parent macrocycle donor (LES) emission. In accordance with the energy gap law, as the emission of the exciplex is pushed to lower energies, vibrational and other nonradiative electronic processes become the primary decay pathways and consequently the quantum yield diminished. In thin films, the absence of solvent interactions attenuates the stabilization of the highly polar complexes and restricted the rotational and translational freedom of the DA pairs. The reduced ability to adopt the lowest-energy configuration resulted in a blue-shift of about 50 nm in the exciplex emission compared to that in the solution fluorescence. Beens and Weller have found that solvent reorganization and relaxation have strong effects when the exciplexes possess dipole moments that correspond to nearly complete electron transfer.[22] Our present solid-state studies are corroborated by our previously reported solvatochromatic exciplex emission[15] that confirms the dominant role of charge-transfer interactions in the electronic structures of the rotaxane exciplexes.[14]

Thermodynamic Considerations. According to Figure 1, the energy of the exciplex emission is given by

$$h\nu_{\text{exciplex}} = \Delta E_{00} - \Delta H_{\text{ex}} - \Delta E_{\text{rep}}$$

The repulsive term, ΔE_{rep}, pertains to the destabilized character

(22) Beens, H.; Weller, A. *Acta Phys. Pol.* **1968**, *34*, 593.

Scheme 1 [a]

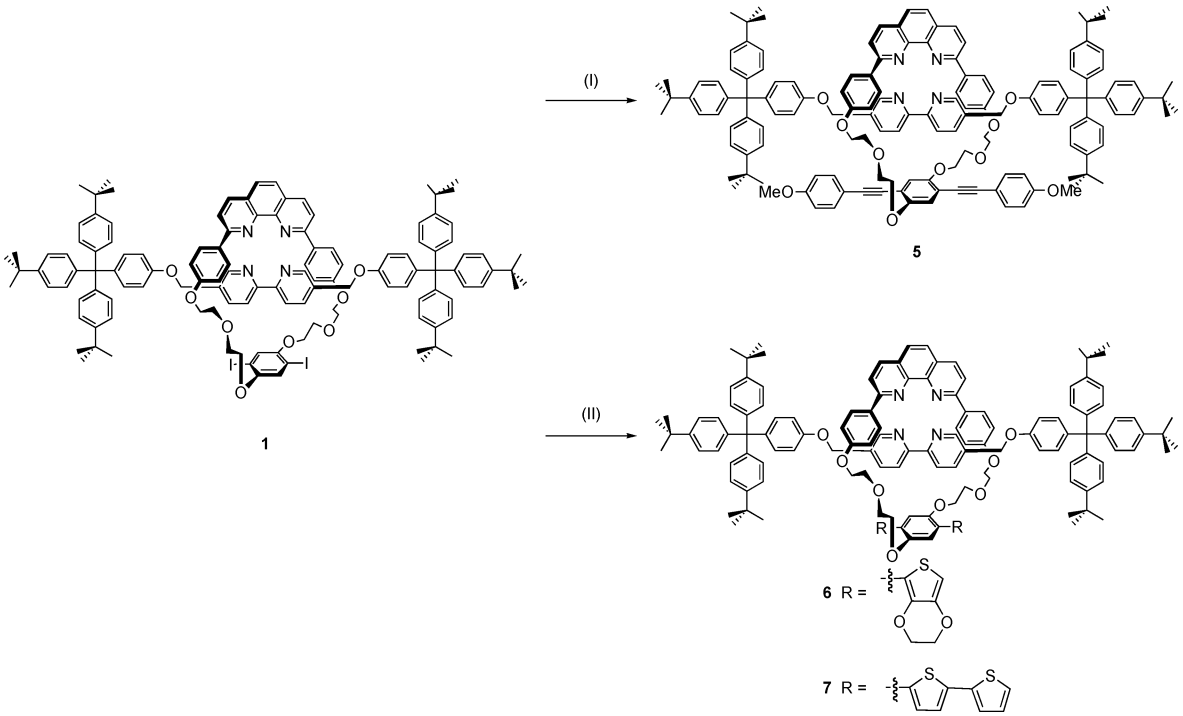

[a] Reaction conditions: (i) *p*-methoxyethynylbenzene, CuI, $Pd(PPh_3)_4$, $PhCH_3$/*i*-Pr_2NH, 60 °C; KCN. (ii) R-$SnBu_3$, CuI, $Pd(PPh_3)_2Cl_2$, NMP, 100 °C; KCN.

Table 1

cmpd	emission max (nm)	Φ (in DCM)	τ (ns)
8	397	0.66[a]	1.5[a,b]
9	394	0.80	1.9[b]
10	397	0.23	1.9[b]
11	466	0.45	1.5[b]
2	526 film: 476	0.02[a]	3.7[a]
3	548 film: 492	0.01[a]	3.9[a]
4	401	0.74	1.6[b]
5	398	0.80	1.6[b]
6	DCM: 399[d], 479 film: 430	0.03	13.8[c]
7	468	0.39	1.5[b]

[a] Previously reported in ref 10. [b] Obtained by phase-modulation method, $\lambda_{exc} = 340$ nm, referenced to a Ludox-water scattering sample. [c] Obtained using streak camera, $\lambda_{exc} = 325$ nm. Monoexponential decay time acquired at 550−600 nm. [d] Contains 1.1% of inseparable impurity, **10**.

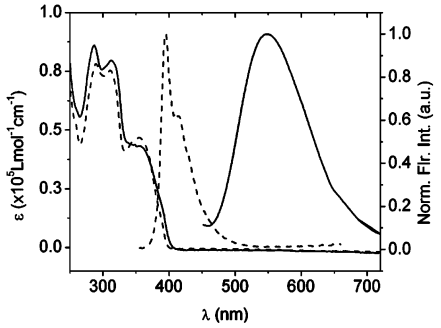

Figure 2. Absorption and emission spectra of rotaxane **3** (solid line, $\lambda_{exc} = 400$ nm) and a mixture of **9** and **12** (dashed line, $\lambda_{exc} = 340$ m) in DCM.

of the ground state in the exciplex geometry immediately after relaxation. Assuming constant ΔE_{rep}, the energy of the exciplex emission increases with decreasing stabilization energy (ΔH_{ex}). This stabilizing term represents the Coulombic attraction and solvation of the charge-separated DA pair. Previous studies on the phenylene−ethynylene-based rotaxanes established the significance of donor and acceptor matching.[15,16] As expected, we observed no interaction between the bipyridine diether threading unit with the oligo(phenylene−ethynylene) donors in rotaxanes **4** and **5**. In rotaxanes **6** and **7**, we incorporated the electron-rich thiophene-based donors in an attempt to offset the inferior electron affinity of the bipyridine diether acceptor. The two oxygen atoms at the 3 and 4 positions of the thiophene ring significantly boost the electron-donating ability of macrocycle **10**. Consequently, rotaxane **6** undergoes excited-state charge transfer that results in exciplex formation. Rotaxane **6** emitted at 493 nm, which is considerably higher energy than those of **2** and **3**, whose emissions were centered at 526 and 548 nm, respectively (Table 1). In addition, the exciplex emission of **6** showed the lowest red-shift (78 nm, 0.51 eV) in relation to the donor LES emission, and it also had the longest excited-state lifetime (13.79 ns). As a reference, we observed a red shift of 150 nm (0.88 eV) and a lifetime of 3.9 ns in rotaxane **3** compared to those for donor **9**. We attribute the reduced stabilization observed in **6** to the weakened charge-transfer interactions between the DA pair. The computer model of macrocycle **10** using AM1 level of calculations reveals torsional strain between the EDOT groups and the center aryl ring in the fluorophore due to steric hindrance. The departure from planarity in the emissive donor undermines the orbital coupling of the DA pair and destabilizes the resulting charge-separated complex. In comparison to donor **10**, the bithiophene-derivatized macrocycle donor **11** possessed a slightly higher oxidation potential, a more diffusive π orbital, and a lower HOMO−LUMO gap of 2.5 eV.[23] Consequently, we observed no exciplex emission in rotaxane **7**.

(23) The HOMO−LUMO gap was obtained from the extrapolated onset of UV−vis absorption. The other three donors (**8**−**10**) have band gaps of ca. 3.1 eV.

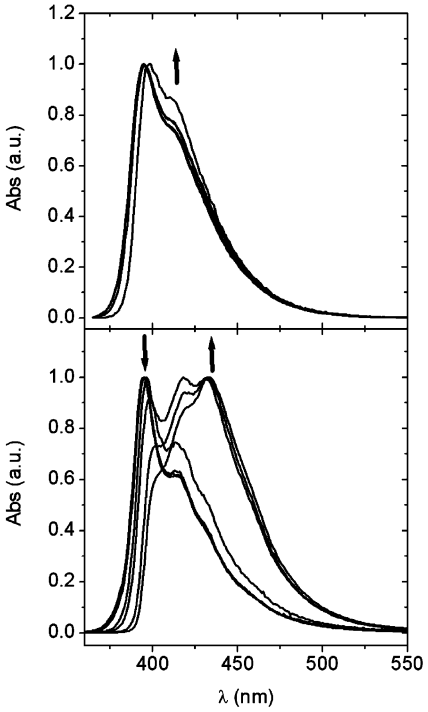

Figure 3. Fluorescence spectra of a **8**/**12** mixture from 1.7 to 170 μM in crements of 24 μM (top) and a **9**/**12** mixture from 1 to 300 μM in increments of 50 μM (bottom) in DCM, $\lambda_{exc} = 340$ nm.

The Effect of Mechanical Confinement of the DA Pair. Although the rotaxane configuration physically confines the donor and acceptor to a distance close enough for $\pi-\pi$ orbital overlap, the two components retain most of their individual rotational and translational freedom. To investigate the effect of this interlocked configuration on the donor and acceptor interactions, we compared the photophysics of donor and acceptor mixtures (not interlocked) to the rotaxane exciplexes and attempted to induce intermolecular exciplex formation by increasing the concentration of the donor and acceptor. We observed no emissive exciplex in mixtures of donors **8** and **12** at any accessible concentrations (1.7−170 μM). However, an equimolar mixture of donor **9** and **12** showed a new emission at 433 nm at concentrations of and above 100 mM (Figure 3). We attributed the exciplex formation to the increased electron-donating ability of the methoxy groups in donor **9**, which supplemented the electrostatic attraction of the exciplex. The exciplexes formed under these conditions were intermolecular in nature and therefore were diffusion limited and concentration dependent. Compared to their intramolecular counterpart, **3**, the intermolecular exciplexes of **9** and **12** emitted at significantly higher energies. These observations suggest that the rotaxane configuration stabilizes the charge-transfer complex. Moreover, the extremely small DA distance (3.5 Å) in the rotaxanes allows for a substantial electronic coupling and a significantly reduced activation energy barrier for exciplex formation. As demonstrated by rotaxane **2**, the stabilizing effect of the rotaxane architecture was strong enough to compensate for the modest thermodynamic driving force for charge-transfer interactions between the DA pair.

Temperature Effects. As stated earlier, the polar nature of the exciplex is the result of charge-transfer character. Upon photoexcitation, a cascade of dynamic processes initiate to stabilize the charge-separated excited state. The donor and acceptor undergo internal reorganization to adopt the most favorable conformation for exciplex formation, while the surrounding solvent molecules also reorganize to stabilize the highly polar complex. In general, lowering the temperature hampers these processes, such that as the rate of charge transfer decreases, the exciplex emission vanishes while the LES emission increases in intensity. In an intramolecular exciplex, however, the pre-organization and conformational restriction of the DA pair complicate the charge-transfer step and can lead to very complex and interesting observations.[24] We examined and compared the exciplex emissions of rotaxanes **2**, **3**, and **6** in butyronitrile at 25 to 50 °C and in a frozen glass at 77 K. Figure 4 illustrates the emission profiles of rotaxane **3** at various temperatures. These results are representative of the other rotaxane exciplexes. With increasing temperature from 25 to 50 °C, the exciplex emission band shifts to shorter wavelengths and decreases in intensity. Interestingly, we observed no LES emission at 77 K. In a frozen butyronitrile matrix, the exciplex emission band is pushed to even higher energies, and its intensity increases by at least an order of magnitude. In a control experiment with the same concentration and solvent, the fluorescence spectrum of the donor and acceptor mixture in an intermolecular fashion revealed only the LES emission from the macrocycle donor. Wang and co-workers observed a similar behavior in (*N*,*N*-dimethylanilino)-CH_2-9-cyanoanthracene, in which a new, blue-shifted emission band is observed at 77 K.[25] By examining the excitation spectra at different emission wavelengths, they attributed the low-temperature emission to a ground-state CT interaction. Figure 5 illustrates the excitation

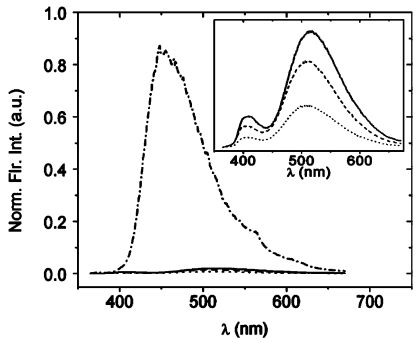

Figure 4. Emission spectra of **3** at room temperature (solid line), 40 °C, (dashed line), 50 °C (dotted line), and 77 K (dash−dot line) in butyronitrile, $\lambda_{exc} = 350$ nm.

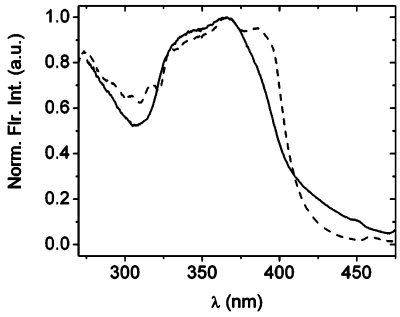

Figure 5. Comparison of excitation spectra of **3** at room temperature (solid line) and 77 K (dashed line) in butyronitrile, $\lambda_{em} = 480$ nm.

(24) Lauteslager, X. Y.; van Stokkum, I. H. M.; van Ramesdonk, H. J.; Bebelaar, D.; Fraanje, J.; Goubitz, K.; Schenk, H.; Brouwer, A. M.; Verhoever, J. W. *Eur. J. Org. Chem.* **2001**, 3105−3118.
(25) Wang, H.; Zhang, B. W.; Cao, Y. *J. Photochem. Photobiol. A: Chem.* **1995,** *92,* 29−34.

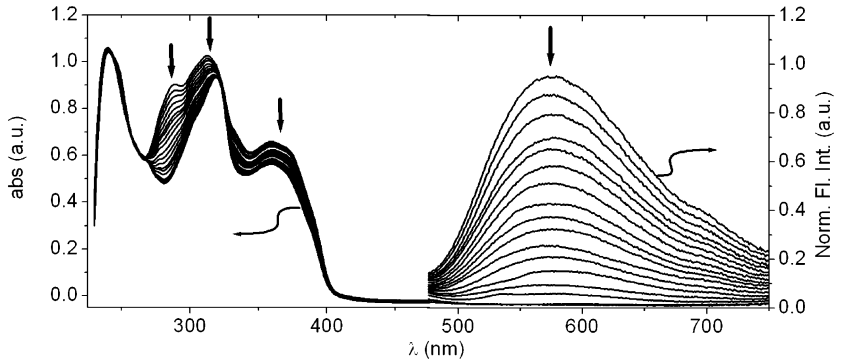

Figure 6. UV−vis absorption (left) and emission (right) titration experiment of 15.2 μM **3** with increments of 0.83 μM $Zn(ClO_4)_2$ in CH_2Cl_2, λ_{exc} = 435 nm.

Table 2. Emission Maxima of Exciplexes at Various Temperatures in butyronitrile and in Solid State

cmpd	λ_{em} rt (nm)	λ_{em} 77 K (nm)	λ_{em} solid-state rt (nm)
2	526	474	476
3	548	495	492
6	479	422, 446	430

profiles of rotaxane **3** at room temperature and 77 K. At low temperature, the excitation spectrum revealed fine vibrational features but otherwise overlaps well with the room temperature excitation. Although the shoulder around 385 nm grows to become a prominent band as the temperature dropped from room temperature to 77 K, it is unclear if the low temperature emission originates from a ground-state CT conformer. Furthermore, in a frozen glass, the exciplex emission resembled the solid-state emission in thin films (Table 2). Freezing the surrounding media of the rotaxane exerts a strong influence on the charge-transfer interactions of the DA pair, and the lack of mobility is analogous to the solid-state environment. In either case, the DA pair and the surrounding solvent molecules lack the flexibility to reorganize and adopt a lowest-energy conformation. The complete absence of LES emission at low temperature further corroborates our hypothesis that pre-organization of the DA pair in a rotaxane architecture dramatically lowered the activation energy barrier for charge transfer.[22] In addition, the striking similarity between the low-temperature emission and the thin film emission suggests that the rotaxane exists as a contact pair exciplex in solution state, in contrast to a solvent-separated complex.

Conformation Effects. The distance and orientation of the DA pair play a critical role in the optical properties of the exciplexes. General theoretical models suggest that the sandwich conformation of the DA pair is optimal for exciplex formation.[26] Because both the donor and acceptor in a rotaxane retain their rotational and translational freedom, one could influence the exciplex optical properties by chemically perturbing their relative conformation. Our group has previously reported that the occupation of the tetrahedral pocket by zinc ions prevents exciplex formation by disrupting the π orbital overlap of the donor and acceptor (Scheme 2).[15] To account for the absence of LES emission, we proposed that the tetrahedral zinc complex allows facile energy- or electron-transfer quenching.[15] For rotaxanes **2** and **3**, binding of alkali, alkali earth, and first-row transition metal ions (Cu^+ and Zn^+) resulted in a linear

Scheme 2. Exciplex Emission Quenching via Conformational Perturbation

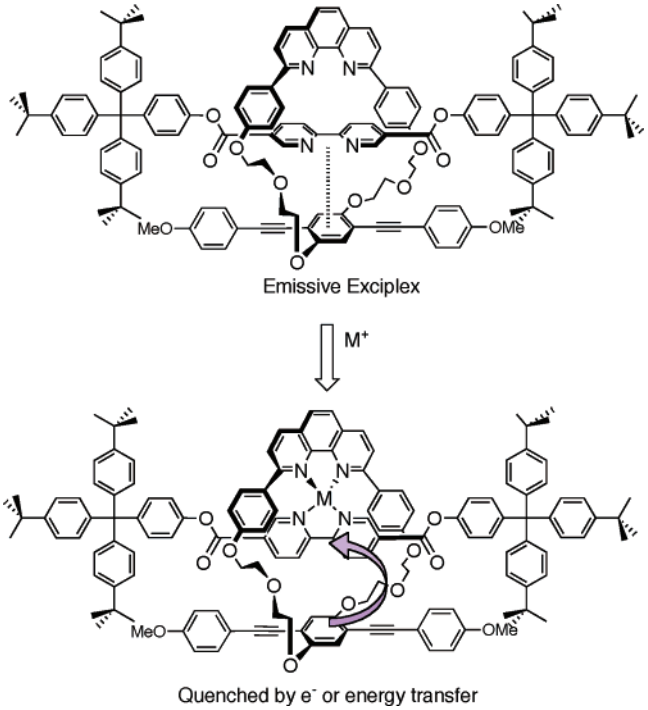

diminution of the exciplex fluorescence (Figure 6). Binding of rotaxane **6** to group 2 and first-row transition metal ions resulted in similar quenching behavior (Figure 7). However, when exposed to alkali metal ions (Li^+ and Na^+), a new and further red shifted emission band (570 nm for Li^+, 558 nm for Na^+) emerged with the concomitant attenuation of the exciplex emission band centered at 493 nm (Figure 7). The minor emission at 400 nm originates from the residual LES emission from approximately 1.1% of the inseparable macrocyclic impurity **10**.[27] UV−vis titration experiments of rotaxane **6** with Mg^{2+}, Cu^+, Cu^{2+}, and Zn^{2+} revealed the disappearance of the absorption band at 286 nm, which is ascribed to the phenanthroline absorption, while Li^+ or Na^+ binding caused a slight attenuation and red-shift of the absorption band to 290 nm

(26) (a) Brouwer, F. Structural Aspects of Exciplex Formation. In *Conformational Analysis of Molecules in Excited States*; Waluk, J., Ed.; Methods in Stereochemical Analysis; Wiley-VCH: New York, 2000; p 204. (b) De Schryver, F. C.; Collart, Pl; Vanderdriessche, J.; Goedeweeck, R.; Swinnen, A.; Van der Auweraer, M. *Acc. Chem. Res.* **1987**, *20*, 159−166.

(27) The impurity emission was detectable after subjected to repeated recrystallization and column chromatography. Because of the high quantum yield of the macrocycle relative to that of the exciplex (Table 1), even a minuscule amount of the macrocycle present can overwhelm the emission spectrum of the exciplex. Analysis of the emission spectrum shows that about 1.1% of macrocycle **10** is present in the sample. We observed similar trends in all rotaxane exciplexes. But unlike other rotaxane exciplexes, the sensitivity of **6** made it unsuitable for the rigorous purification procedures we usually utilized.

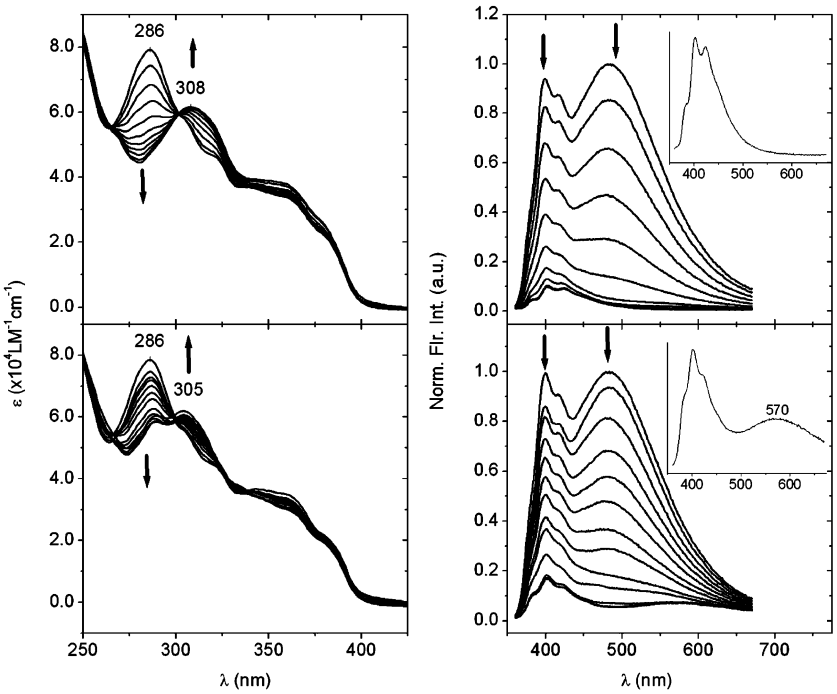

Figure 7. (Top) UV−vis absorption (left) and emission (right) titration of **6** with increments of 0.59 μM $Zn(ClO_4)_2$ in CH_2Cl_2. (Bottom) UV−vis absorption (left) and emission (right) titration of **6** with increments of 0.46 μM $Li(ClO_4)$ in CH_2Cl_2. Concentrated of **6** stock solution = 5.0 μM. λ_{exc} = 350 nm. (Inset) Emission spectrum of rotaxane at excess metal ion concentration.

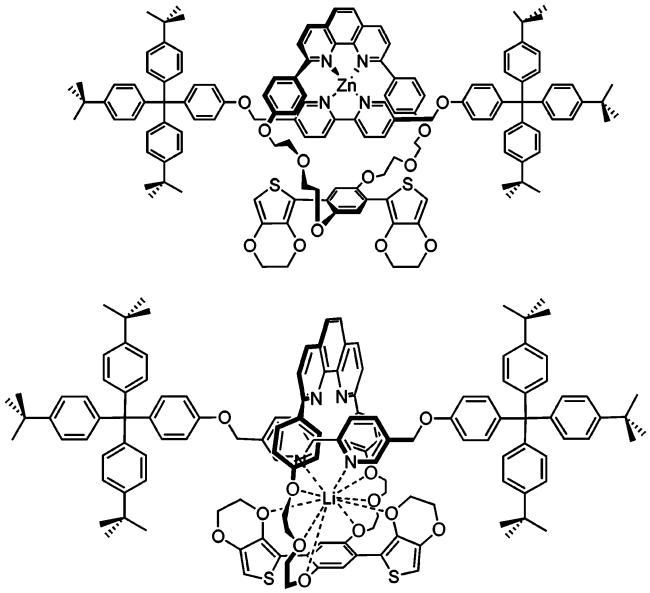

Figure 8. (Top) Tetrahedral binding of Zn^{2+} to rotaxane **6**. (Bottom) Proposed stabilization of Li^+ by the oxygen atoms in the lower rim of rotaxane **6**.

(Figure 8). The different absorption profiles suggest two distinct binding motifs. The "hard" alkali metal ions favor chelation to the hard Lewis basic oxygen atoms on the ethylene glycol linker and on the EDOT rings. On the other hand, the soft transition metal ions exhibit less flexibility to depart from the tetrahedral coordination environment and prefer binding to the nitrogen-containing aromatic groups, which are softer Lewis bases and capable of having a π orbital contributing to the bonding. We therefore conclude that alkali metal ions chelate to the lower rim of the rotaxane so as to interact with the oxygen atoms of ethylene glycol linkers and the EDOT rings. Figure 8 illustrates the two sites for metal coordination. The broad and featureless emission profile of the resulting complex suggests a new excited-state species with charge-transfer character, although the conformation of the complex and the mechanism of the interaction remain unclear.

Conclusions

We have shown that physical confinement of a donor and an acceptor in a rotaxane architecture profoundly influences the optical properties of the resulting exciplex. By introducing EDOT moieties into the donor, we have demonstrated that the improved electron donating ability of the donor offsets the inferior electron affinity of the bipyridine diether acceptor and leads to exciplex emission. In addition, the preorganization of the rotaxane-bound DA pairs substantially lowers the activation energy barrier for exciplex formation, as demonstrated by the intermolecular model experiments and temperature dependence studies. Metal binding to the tetrahedral pocket of the rotaxane freezes the relative DA conformation and quenches the exciplex fluorescence. Coordination of alkali metal ions (Li^+ and Na^+) to the EDOT-based rotaxane results in the emergence of a weaker and further red shifted emission. From the UV−vis titration experiments, we conclude that the alkali metal ion occupies a different binding site and produces a new emissive species. These results reveal the diversity of supramolecular photophysics that opens new doors for the utilization of supramolecular complexes in future molecular chemosensor and optoelectronic device development.

Note Added after ASAP Publication. There were errors in the captions of Figures 2 and 7 and in the references to Figures 6 and 7 in the version published ASAP on March 15, 2005. The correct version was posted March 28, 2005.

Acknowledgment. We thank ONR and DOE for funding this work. We also thank Mr. Justin Hodgkiss for assistance and advice with the streak camera lifetime experiments.
JA042535O